Responses to reviews of "Observations of XCO_2 and XCH_4 with ground-based high-resolution FTS at Saga, Japan and comparisons with GOSAT products" by H. Ohyama et al.

Anonymous Referee #2

This paper introduces the Saga TCCON station, the first 2.5 years of its operation, the particular environment in which it is located, and the relationship between its data and the GOSAT TANSO-FTS data. The paper discusses the impacts of the origin of air on the retrievals from the TCCON station, and the impacts of aerosol and high cirrus on the TANSO-FTS retrievals. It is suitable for publication in AMT after revisions.

We thank you for reading our paper carefully and providing valuable comments. Detailed responses to your comments are included below and indicated in red. We revised our manuscript according to the comments and added some detailed explanations. Please see our specific responses below.

General comments:

A major result from this paper is that the TANSO-FTS retrievals are significantly affected by aerosol and high cirrus, but this discussion is very short and incomplete. This section needs to be fleshed out, showing statistical significance, and including supporting plots for the statements that the biases are of a different sign for different aerosol types.

We made a new subsection (Sect. 4.5) that is dedicated to describing aerosol-induced effects on the TANSO-FTS XCO_2 and XCH_4 retrievals. In the first paragraph of Sect.

4.5, we added the following sentences: "*t*-values of statistical *t*-test are 2.4 and 0.66 (the number of data point n = 90) for XCO_2 and XCH_4, respectively, suggesting the correlation is significant for only XCO_2 at 95% confidence. Meanwhile, the differences between TANSO-FTS and g-b FTS data are independent of the Ångström exponent, which is a measure of the size of the aerosol particles, for both XCO_2 and XCH_4."

Moreover, we revised the second paragraph of Sect. 4.5 as follows:

"Next, the effects of aerosol and cirrus profiles on the TANSO-FTS XCO_2 and XCH_4 retrievals were investigated using data measured with a lidar at Saga (Uchino et al., 2012b). The total number of coincidence measurements with the g-b FTS, TANSO-FTS, and lidar at Saga was 31. On the basis of vertical profiles of the backscattering ratio (R) and total depolarization ratio at 532 nm (Dep.), and of the backscatter-related wavelength exponent between 532 and 1064 nm (Alp), which were measured with the lidar, we categorized the state of the atmospheric particulates (aerosol/cloud) into three types (tropospheric aerosol, cirrus cloud, and low cloud). The tropospheric aerosol was further categorized into large-AOD tropospheric aerosol and normal tropospheric aerosol (clear sky), depending on whether an AOD measured with the lidar was larger or smaller than 0.5. The numbers of the respective types resulted in 4 for the large-AOD tropospheric aerosol, 19 for the normal tropospheric aerosol, 4 for the cirrus cloud, and 4 for the low cloud. Since the low cloud scenes were likely cloudy just within the lidar receiver field of view (FOV) and was clear within the TANSO-FTS instantaneous FOV, the low cloud scenes were not treated. If only the normal tropospheric aerosol scenes were considered, the correlations of the difference between TANSO-FTS and g-b FTS data and the AOT values are not significant for XCO_2 as well as for XCH_4. Therefore, the large-AOD tropospheric aerosol and the cirrus cloud

would cause the negative correlation. We present distinctive case studies relevant to the large-AOD tropospheric aerosol and the cirrus cloud, and their overall impacts on the XCO_2 and XCH_4 retrievals, since there are not enough number of data for the large-AOD tropospheric aerosol and cirrus cloud scenes to statistically show the relationship between the particulate types and the differences in XCO_2/XCH_4 between TANSO-FTS and g-b FTS.

Figures 10a and b show vertical profiles of the R, Dep., and Alp. Aerosols on 29 May 2012 in Fig. 10a were uniformly distributed below a height of 3 km and the AOD for 0–10 km was large (i.e., 1.28, assuming an aerosol extinction-to-backscatter ratio of 50 sr). For this large-AOD tropospheric aerosol scene, the differences between TANSO-FTS data closest to the Saga site and g-b FTS data are −4.82 ppm for XCO_2 and −7.2 ppb for XCH_4. The mean biases for the large-AOD tropospheric aerosol scenes are –1.36 ± 1.96 ppm for XCO_2 and –9.9 ± 7.7 ppb for XCH_4. On 8 November 2013 shown in Fig. 10b, thin cirrus clouds was observed around 8.5 km and the AOD was 0.018 assuming an aerosol extinction-to-backscatter ratio of 20 sr. Total AOD, including aerosols below 2 km was 0.49 for the altitude range of 0–15 km. The differences between TANSO-FTS data closest to the Saga site and g-b FTS data are 4.01 ppm for XCO_2 and 19.5 ppb for XCH_4. The mean biases of XCO_2 and XCH_4 for the cirrus cloud scenes are 2.04 ± 2.17 ppm and –1.0 ± 12.0 ppb, respectively. The differences between the mean biases for the large-AOD tropospheric aerosol and cirrus cloud scenes are significant for XCO_2 and not significant for XCH_4. It is unclear what made the XCO_2 retrieval sensitive (or the XCH_4 retrieval insensitive) to the particulate type. While the difference in the spectral range practically used for the retrieval (XCO_2: Band 1-3; XCH_4: Band 1-2) might affect the retrieval results, further investigations are

necessary to figure out the cause. As a whole, effects of aerosols/cirrus clouds on the TANSO-FTS XCO_2 retrievals result in a weak negative correlation of the differences between TANSO-FTS and g-b FTS data against AOT as well as in a large scatter of TANSO-FTS data. We note that the effects of the difference in aerosol type on the XCO_2 and XCH_4 retrievals would be dependent on treatment of aerosol profile in each retrieval algorithm. A treatment of cirrus clouds in the TANSO-FTS NIES XCO_2 and XCH_4 retrievals will be incorporated in the next version of the Level 2 algorithm (Y. Yoshida, private communication)."

The analysis of the back-trajectories and their impacts on the relationships between $\Delta XCO/\Delta XCO_2$ and $\Delta XCH_4/\Delta XCO$ needs more discussion. Why lump all the summertime data together and fit it with a single line (dashed lines in Fig 6)? What can you learn by fitting the different regions (types I–III) separately? Can you compare the relationships with known emissions factors for the three regions? If the data are dense enough, how does the seasonal cycle using only the type I data compare with the entire time series (wrt the trends, seasonal cycle amplitudes, etc.)?

In the revised manuscript, the types I–III data in the summertime were separately fitted. The respective fitted lines were inserted into Figs. 6a and 6b, and Table 3 that summarizes correlation coefficients and slopes of $\Delta XCO/\Delta XCO_2$ and $\Delta XCH_4/\Delta XCO$ was added. In addition, we revised the second and third paragraphs of Sect. 4.3 as follows:

"Figures 6a and b show correlation plots of $\Delta XCO/\Delta XCO_2$ and $\Delta XCH_4/\Delta XCO$, respectively, whose values are represented by the daily mean values. Figures 5b and 6a indicate that most of the low-XCO_2 events in the summer season are

driven by long-range transport of air masses associated with strong biospheric uptake over the Asian continent (type I). Wada et al. (2007) reported that low-CO_2 events at ground level in the summer season were observed at Minamitorishima (24.3°N, 154.0°E, Fig. S6) in the Northwest Pacific. We note that the air masses passing over Saga are expected to travel toward Minamitorishima. With regard to XCO, high-XCO events correspond to transport of air masses from the Asian continent (type I) or Southeast Asia (type II), while low-XCO events correspond to air mass transport from the Pacific Ocean (type III). The slope of the $\Delta XCO/\Delta XCO_2$ ratio for the type I is negatively gentler than for the type II, and that is due to the transport of the air masses that experienced the strong biospheric uptake of CO_2 over the Asian continent (i.e., negatively larger ΔXCO_2 for the type I). However, statistical *t*-test indicates that the correlation for the type I as well as the type III is not significant at 95% confidence. For the winter season, it is probable that the burning of fossil fuel causes the positive steep slope of the $\Delta XCO/\Delta XCO_2$ ratio.

As shown in Fig. 6b, the slopes of the $\Delta XCH_4/\Delta XCO$ ratio for the summer season are steeper than that for the winter season, and the differences between the types I-III for the summer season are smaller than the differences between the summer and the winter seasons. The differences in the slopes for the types I-III are statistically insignificant. The slope of the $\Delta XCH_4/\Delta XCO$ ratio for the type III is formed from the air masses with the lowest values for both ΔXCH_4 and ΔXCO, which were transported from the Pacific Ocean, where CH_4 and CO emissions are low. The slope of the $\Delta XCH_4/\Delta XCO$ ratio for the type II is attributable to the air masses with the highest ΔXCH_4 and ΔXCO values, which were transported from Southeast Asia, where CH_4 emissions from rice fields significantly increase during the summer (Bergamaschi et al.,

2009) and CO concentrations are high (Worden et al., 2010). Consequently, the slopes of the $\Delta XCH_4/\Delta XCO$ ratio for the types I-III become almost equivalent. For the winter season, although the ΔXCO values remain high, the decrease in CH_4 emissions over Asia during the winter causes the gentle slope of the $\Delta XCH_4/\Delta XCO$ ratio."

Moreover, we executed the fitting procedure described in Sect. 4.2 for the time series of only the type I data. The seasonal cycle amplitudes for XCO_2 changed from 6.9 to 8.0 ppm, and the seasonal cycle amplitudes for XCH_4 and XCO showed little change. The growth rates (trends) resulted in 2.4 ppm yr^{-1}, 8.0 ppb yr^{-1}, and –1.9 ppb yr^{-1} for XCO_2, XCH_4, and XCO, respectively. We added the following sentences in the last paragraph in Sect. 4.3: "If the fitting procedure described in Sect. 4.2 was performed for only the type I data, the growth rates were 2.4 ppm yr^{-1}, 8.0 ppb yr^{-1}, and –1.9 ppb yr^{-1} for XCO_2, XCH_4, and XCO, respectively. Compared to the case of using the entire data, the growth rate of XCO_2 increased and those of XCH_4 and XCO decreased. This would support the guess concerning the emissions in the continental area."

Table 3. Correlation coefficients and slopes of $\Delta XCO/\Delta XCO_2$ and $\Delta XCH_4/\Delta XCO$. The correlation coefficients and slopes for DOY 170-260 are indicated separately for types I-III.

	$\Delta XCO/\Delta XCO_2$		$\Delta XCH_4/\Delta XCO$	
Period/Trajectory type	Correlation coefficient	Slope [ppb ppm^{-1}]	Correlation coefficient	Slope [ppb ppb^{-1}]
DOY 1-90	0.62	16.6	0.91	0.84
DOY 170-260 Type I	–0.34	–3.15	0.80	1.04
DOY 170-260 Type II	–0.52	–14.3	0.92	1.08
DOY 170-260 Type III	–0.04	–0.52	0.86	1.14

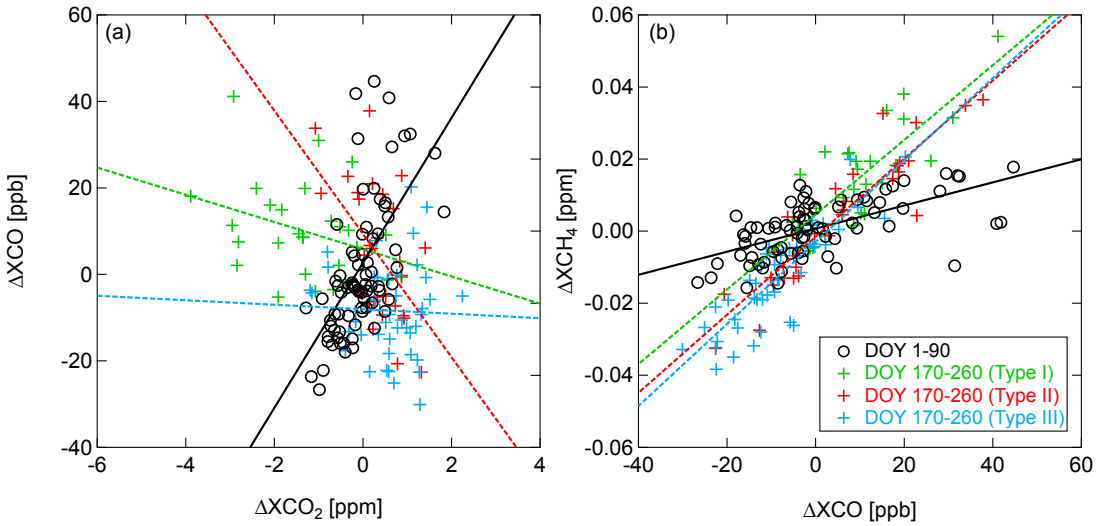

Figure 6 (revised figure)

Please include a map of all the locations you mention in the paper: Saga, Heteruma Island, Minamitorishima Island, Fukue Island, etc.

We added a map of all the locations mentioned in this paper (Saga, Hateruma Island, Minamitorishima, Fukue Island, and Tsukuba) in the supplementary material.

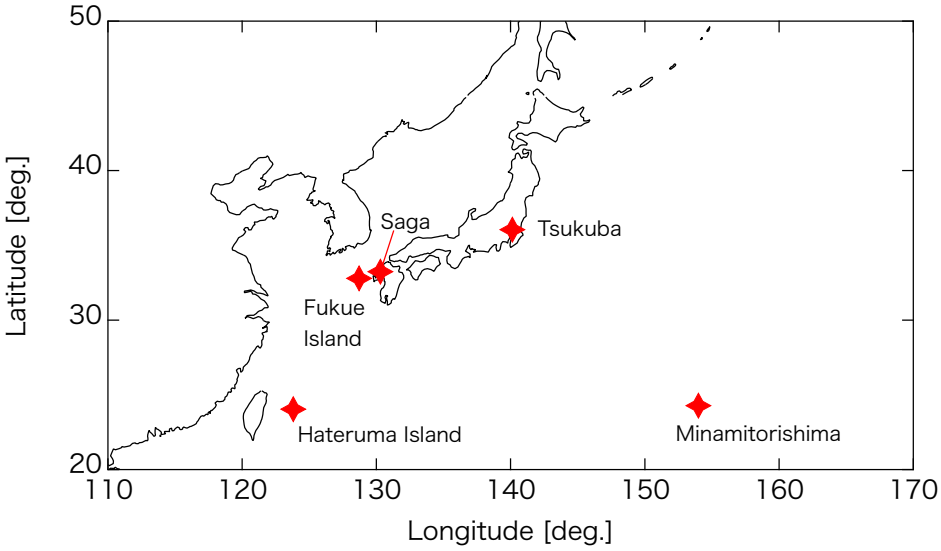

Figure S6. A map of all the locations mentioned in the text.

Technical comments (suggested changes between **):

P8259L22: tend to *cause an* overestimate or underestimate *in* the TANSO-FTS *retrievals*.

We revised accordingly.

P8260L9: move the Chevallier et al. citation to after "of CO_2"

We revised accordingly.

P8260L13: instead, try: space-based instruments*: the* Scanning...

We revised accordingly.

P8260L22: You're missing several references: Morino et al., Butz et al., Wunch et al. 2011.

We added the three references in the revised manuscript.

P8261L1: replace "under" by "following"

We revised accordingly.

P8261L4: remove "derived"

We revised accordingly.

P8264L5: Suggest adding the following sentence: "We use the standard implementation of GGG for TCCON retrievals, described briefly below."

We revised accordingly.

Section 3.2 describes a screening method that does not conform to the TCCON standard. The screening on the pyranometer should no longer be necessary for GGG2014, as the fractional variation in solar intensity is now calculated from the interferograms themselves. Please comment on how the standard TCCON screening compares with yours.

We added the following sentences: "We compared this screening method with the other one using only the interferograms, which was added to GGG2014 and adopted for several TCCON sites. Figure S4 shows the time series of XCO_2 for the respective screening methods, and Fig. S5 shows the numbers of data per month. From these comparisons, we found that the screening method used in the present study is conservative."

We are thinking of the use of the SIV calculated in GGG in future (from next version of GGG software).

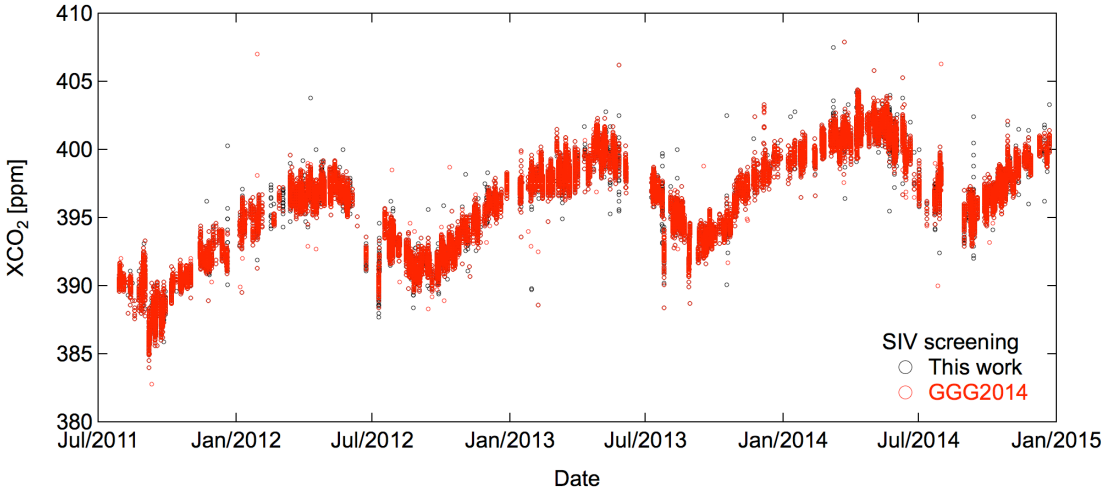

Figure S4. Time series of XCO_2 based on the screening methods used in this work (black) and calculated in GGG2014 (red).

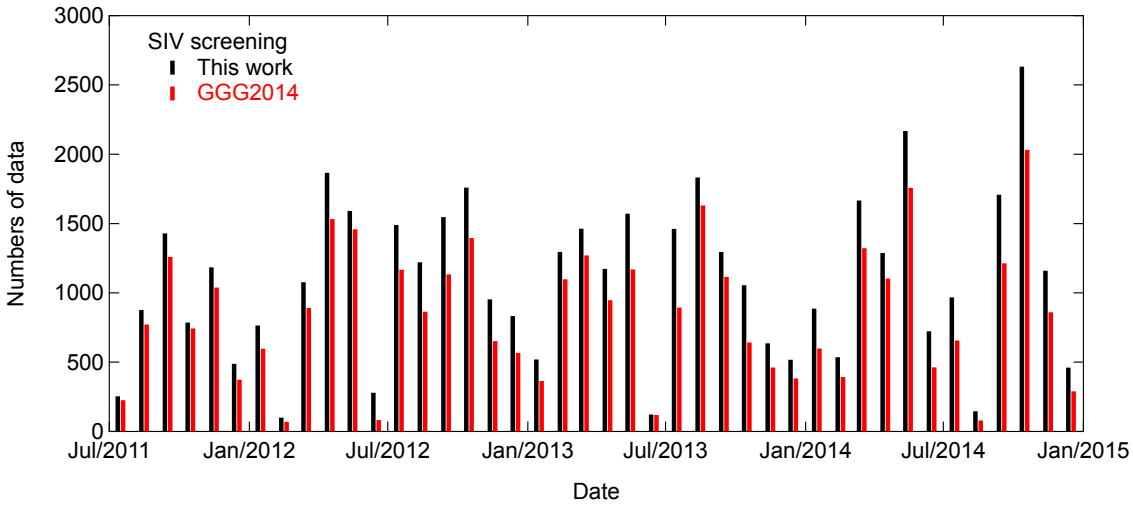

Figure S5. The numbers of data per month based on the screening methods used in this work (black) and calculated in GGG2014 (red).

The screening based on solar zenith angles less than 70 due to the interface between the glass and polyvinyl is reasonable, but it should be clearly stated that this differs from the typical TCCON screen (82 degrees).

We revised the sentence as follows: "Therefore, we adopted a criterion that the SZA has to be ≤70 degrees rather than ≤82 degrees, which are adopted for the typical TCCON data."

P8266L6: missing reference: Geibel et al.

We added the reference in the revised manuscript.

P8267L20: missing space between FTS and XCO_2.

We revised accordingly.

P8267L23: form –> from

We revised accordingly.

P8268L9: You estimate the error from the difference in tropopause height. What is an estimated error from assuming that the BL and free-troposphere profile above the aircraft is constant? I believe you are underestimating your total errors.

In the revised manuscript, we estimated the total aircraft XCO_2 and XCH_4 errors, and we added the following sentences: "The error components below the maximum flight altitude were estimated by adding twice the precision of the aircraft data to the profile and re-integrating the profile (Wunch et al., 2010): 0.54 ppm for XCO_2 and 6.1 ppb for XCH_4. The stratospheric errors in the aircraft XCO_2 and XCH_4 were estimated by shifting the a priori profile by 1 km: 0.19 ppm for XCO_2 and 7.1 ppb for XCH_4. The total errors were calculated as the root sum squares of the three errors, and we estimated the total errors in the aircraft XCO_2 and XCH_4 to be 0.66 ppm and 9.6 ppb, respectively."

P8268L20: 6-month (no "s") periods were employed to represent seasonal variation, ** low-pass filters with a 2-year cutoff frequency *were used* for the long-term trend*,* and a 150-day cutoff frequency *was used* for the short-term trend.

We revised.

P8268L22-24: I'm confused by the distinction between the filtered datasets and long-term trends. Please clarify.

We revised the first sentence as follows: "The summation of the harmonic functions and the long- and short-term trends is treated as the fitting curve of XCO_2."

Fig 5: Please write the type numbers for each color in the caption.

We added the following sentence to the caption of Fig. 5: "The numbers of trajectory corresponding to type I (green), type II (red), and type III (blue) are 28, 30, and 45, respectively."

References:

Butz, A., S. Guerlet, O. Hasekamp, D. Schepers, A. Galli, I. Aben, C. Frankenberg, J. M. Hartmann, H. Tran, A. Kuze, G. Keppel-Aleks, G. C. Toon, D. Wunch, P. O. Wennberg, N. M. Deutscher, D. Griffith, R. MacAtangay, J. Messerschmidt, J. Notholt, and T. Warneke (2011), Toward accurate CO_2 and CH_4 observations from GOSAT, Geophys. Res. Lett., 38(14), 2–7, doi:10.1029/2011GL047888. Available from: http://www.agu.org/pubs/crossref/2011/2011GL047888.shtml

Geibel, M. C., J. Messerschmidt, C. Gerbig, T. Blumenstock, H. Chen, F. Hase, O. Kolle, J. V. Lavrič, J. Notholt, M. Palm, M. Rettinger, M. Schmidt, R. Sussmann, T. Warneke, and D. G. Feist (2012), Calibration of column-averaged CH_4 over European TCCON FTS sites with airborne in-situ measurements, Atmos. Chem. Phys., 12, 8763–8775, doi:10.5194/acp-12-8763-2012. Available from: www.atmos-chem-phys.net/12/8763/2012/

Morino, I., O. Uchino, M. Inoue, Y. Yoshida, T. Yokota, P. O. Wennberg, G. C. Toon, D. Wunch, C. M. Roehl, J. Notholt, T. Warneke, J. Messerschmidt, D. W. T. Griffith, N. M. Deutscher, V. Sherlock, B. J. Connor, J. Robinson, R. Sussmann, and M. Rettinger (2011), Preliminary validation of column-averaged volume mixing ratios of carbon dioxide and methane retrieved from GOSAT short-wavelength infrared spectra, Atmos. Meas. Tech., 4(6), 1061–1076, doi:10.5194/amt-4-1061-2011. Available from: http://www.atmos-meas-tech.net/4/1061/2011/